AIAA 80-0775R

Interfacial Cracks in Adhesively Bonded Scarf Joints

S. S. Wang* and J. F. Yau†
University of Illinois, Urbana, Ill.

The interfacial crack behavior in adhesively bonded scarf joints is investigated. The study is conducted by using a method of analysis formulated on the basis of conservation laws of elasticity for nonhomogeneous solids and fundamental relationships in fracture mechanics of interfacial cracks. Solutions for interfacial crack-tip responses are determined for the joints with various adherend and adhesive properties, interface crack lengths, and adhesive-layer thicknesses. Also studied is the change of structural stiffness due to the presence of interfacial debonding. Of particular interests are the effects of geometric and material variables on the crack-tip response. Results are presented in terms of mixed-mode stress intensity factor solutions and energy release rates to illustrate the fundamental nature of fracture in adhesively bonded scarf joints.

I. Introduction

APPLICATIONS of adhesive joining technology to advanced engineering structures such as aircraft construction have been of significant interest recently. Although adhesive joints have been employed in many secondary structural components, the reliable and effective use of adhesively bonded joints for primary load-bearing structures still remains in its infancy. The major factors responsible for this situation are the complex failure modes and mechanics presented in the joints. Among the various kinds of failure problems in adhesively bonded structures, interfacial cracking, sometimes also called debonding, often causes the greatest concern because it is one of the most commonly encountered failure mechanisms in the joints. Interfacial cracks are frequently observed to occur in fabrication and manufacturing processes such as trapped air bubbles or incomplete wetting between an adhesive and adherends. The cracks are also found to be initiated at geometric and material discontinuities such as at the edge of an adhesive-adherend interface. The presence of interfacial cracks in an adhesive joint can result in a progressive reduction of joint stiffness, the exposure of the interior of the composite to environmental attack, and the disintegration of the structure, which leads to the final fracture. Thus, understanding the basic nature of interfacial cracks and the ability of analyzing this critical problem are of paramount importance in the reliable design and future applications of the joints for primary load-bearing structures.

The scarf joint, which is considered to provide a higher strength than a lap-shear joint,[1] is studied because it is one of the most widely used configurations in transferring loads. Due to the complex structural geometry, the presence of a nonhomogeneous material system, the singular nature of debonding along the interface of dissimilar materials, and the unknown multiaxial stress state acting on the crack, the interfacial crack problem in adhesively bonded scarf joints is obviously very difficult. The very localized nature of the crack-tip response, as shown in Refs. 2-5, introduces the bond thickness as a characteristic dimension in the problem. Any simplifications that fail to include the thin but critically important adhesive layer would be unwise. The importance and complexities of interfacial debonding in adhesive joints have long been recognized[6-9]; however, research progress has been relatively slow due to the aforementioned difficulties. In this paper a rigorous study of the mixed-mode interfacial crack problem in the composite structure is presented by using an approach recently developed by the authors.

The loading condition and the geometry of an adhesively bonded scarf joint under investigation are shown in Fig. 1a. The joint is composed of two high-stiffness and high-strength adherends bonded by a thin adhesive layer along a scarf angle ϕ with respect to the applied nominal stress σ_∞ (Fig. 1b). The thin adhesive layer has elastic properties of E_I and ν_I. The two adherends are made of high-modulus metals with material constants E_2, ν_2 and E_3, ν_3. In this study, both the adhesive and the adherends are assumed to be linear elastic. The adhesive layer has a uniform thickness t; the two adherends are considered to have the same uniform thickness d, and the joint, a total length of $2L$. A crack of length a is initiated at the traction-free edge and located along the interface between the adhesive and adherend. Except for the debonding region, the adherends and the adhesive are assumed to be perfectly bonded everywhere along bimaterial interfaces.

The objectives of this research are to: 1) develop an accurate and efficient method of analysis for examining the basic nature of the adhesive joint fracture problem; 2) investigate the complex failure modes and mechanics of interfacial cracks in adhesively bonded scarf joints; and 3) determine the effects of geometric and material variables on the crack behavior in the bonded composite structures.

The method of analysis is formulated on the basis of the recently developed conservation laws of elasticity for nonhomogeneous solids[10-12] and fundamental relationships in fracture mechanics of interfacial crack problems. The interfacial crack-tip response, characterized by inherently mixed-mode crack-tip stress intensity factors, is related to the conservation integrals derived in the paper. The conservation integrals can be evaluated conveniently by using properly introduced auxiliary solutions and field variables removed from the crack tip. The problem is then reduced to a pair of linear algebraic equations. Stress intensity and fracture energy release rate solutions are determined directly. One of the salient features of the present approach is that the stress intensity solution of an interfacial crack in a scarf joint can be determined accurately and efficiently by information extracted from the far field. The simplicity and accuracy of the current method make it particularly attractive for the present complex fracture problem. In the next section, formulation of conservation integrals for nonhomogeneous solids and their relationships with interfacial fracture mechanics parameters are presented. The solution procedure and the associated computational scheme are given in Sec. III. Solutions are shown in Sec. IV for the adhesively bonded scarf joints with

Presented as Paper 80-0775 at the AIAA/ASME/ASCE/AHS 21st Structures, Structural Dynamics and Materials Conference, Seattle, Wash., May 12-14, 1980; submitted May 28, 1980; revision received Feb. 18, 1981.

*Associate Professor, Dept. of Theoretical and Applied Mechanics.
†Graduate Research Assistant; presently, Research Engineer, Aircraft Engine Group, General Electric Co., Evandale, Ohio.

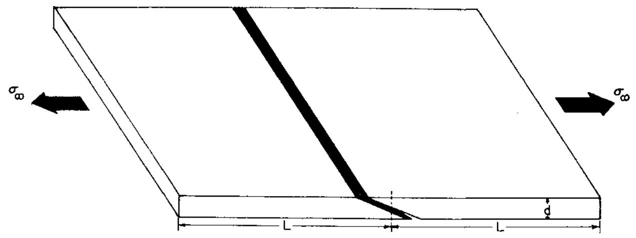

Fig. 1a Adhesively bonded scarf joint with an edge interfacial crack.

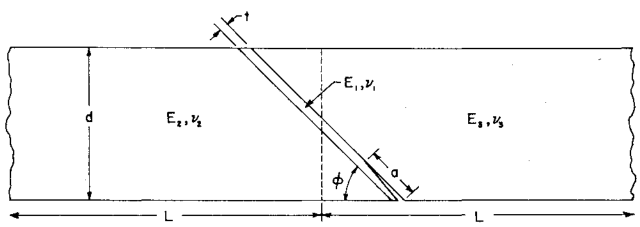

Fig. 1b Geometry and material constants of the joint and the crack.

various materials and geometric variables of the crack and adhesive layer. Many important features of the problem are revealed from the results, and a better understanding of the fundamental nature of the interfacial flaw behavior in adhesively bonded scarf joints is obtained. The method of analysis should be of practical use in a reliable design and analysis of adhesively bonded joints.

II. Basic Formulation

For an infinitesimal deformation of a homogeneous elastic solid, a general form of the Eshelby-Rice conservation law [13-16] in a plane elasticity problem can be written as

$$J_i = \int_S (Wn_i - \sigma_{jk} n_k u_{j,i})\, ds = 0 \tag{1}$$

where W is the strain energy density, σ_{jk} the stress tensor, u_j the displacement vector, and n_i the outward unit normal of an arbitrary closed boundary S which encloses a portion of the continuum. The conservation integral J_i has recently been extended by Smelser and Gurtin [10] to a nonhomogeneous solid composed of dissimilar materials:

$$J_i = \int_S (Wn_i - \sigma_{jk} n_k u_{j,i})\, ds - \int_\ell ([W]\delta_{i2} - \sigma_{j2}[u_{j,i}])\, ds = 0 \tag{2}$$

where ℓ is a portion of the interface bounded by S as shown in Fig. 2a and the brackets denote the jump of a function across $x_2 = 0$, that is,

$$[W] = W(x_1, 0^+) - W(x_1, 0^-) \tag{3}$$

and

$$[u_{j,i}] = u_{j,i}(x_1, 0^+) - u_{j,i}(x_1, 0^-) \tag{4}$$

Continuity conditons of displacements and normal and shear stresses across the interface $x_2 = 0$ require

$$[u_j] = 0 \quad \text{and} \quad [\sigma_{j2}] = 0 \tag{5}$$

Hence, the J_1 component of the conservation integral in Eq. (2) can be simplifed as

$$J_1 = \int_S (Wn_1 - \sigma_{jk} n_k u_{j,1})\, ds = 0 \tag{6}$$

which is the same as the analogous result for a single-phase material.

Consider a solid with a sharp crack located along the interface of two dissimilar materials, as shown in Fig. 2b. For the interfacial crack problem, the conservation integral of Eq. (6) can be shown to have the same form as the well-known J integral of fracture mechanics for monolithic solids without change, i.e.,

$$J \equiv J_1\{\Gamma\} = \int_\Gamma \left(W dx_2 - T_i \frac{\partial u_i}{\partial x_1} ds \right) \tag{7}$$

where Γ is an arbitrary path surrounding the crack tip, provided that the crack surfaces are free from traction and the interface is a straight line. It can also be shown that the J is equal to the energy release rate in the interface crack problem in a usual manner. Define the interfacial crack-tip stress intensity factors, K_I and K_{II}, by

$$K_I - iK_{II} = 2\sqrt{2}\pi e^{\beta\pi} \lim_{z \to 0} z^{1/2 + i\beta} \Phi_1(z) \tag{8}$$

where $\Phi_1(z)$ is a complex potential in the well-known Kolosov-Muskhelishvili's formulation. [8,17] The β in Eq. (8) is the bimaterial constant

$$\beta = \frac{1}{2\pi} \ln \left[\frac{(3-\nu_1)/[G_1(1+\nu_1)] + 1/G_2}{(3-\nu_2)/[G_2(1+\nu_2)] + 1/G_1} \right] \tag{9}$$

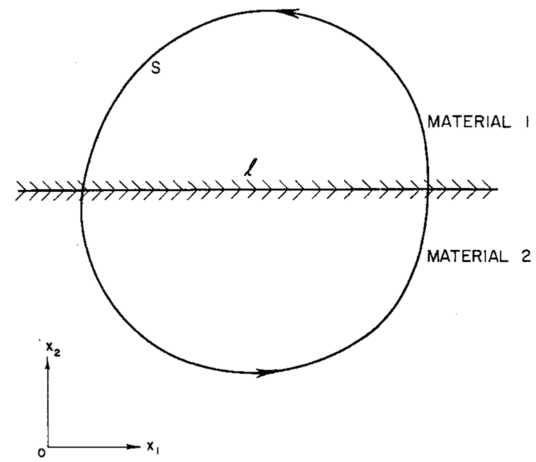

Fig. 2a Closed integration path S for J_i in bimaterial composite.

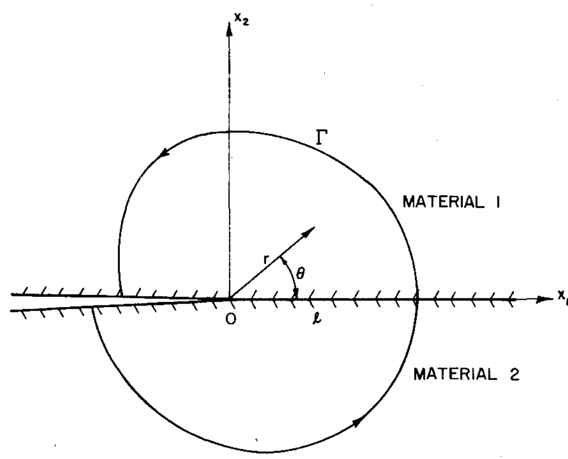

Fig. 2b Interfacial crack between dissimilar adherend and adhesive, and contour path Γ for J and M integrals.

for a plane stress problem, whete G_i and ν_i are the shear modulus and Poisson's ratio of the ith material, respectively. For a plane strain case, ν_i in Eq. (9) is replaced by $\nu_i/(1-\nu_i)$. One can easily show[12,18] that the J integral is related to stress intensity factors of an interfacial crack by

$$J=\mathcal{G}=\alpha(K_I^2+K_{II}^2) \tag{10}$$

where $\mathcal{G}$ is the total energy release rate defined by

$$\mathcal{G}=\mathcal{G}_I+\mathcal{G}_{II} \tag{11}$$

and α has the form

$$\alpha=\begin{cases} \displaystyle\sum_{i=1}^{2} \frac{1}{4G_i}(1-\nu_i) & \text{(plane strain)} \\ \\ \displaystyle\sum_{i=1}^{2} \frac{1}{4G_i(1+\nu_i)} & \text{(plane stress)} \end{cases} \tag{12}$$

Equation (10) was first given by Malyshev and Salganik.[18] The J integral *alone* does not provide adequate information for determining the individual values of K_I and K_{II} in an inherently mixed-mode interfacial fracture problem. However, if Eq. (10) is used in conjunction with conservation integrals for two independent equilibrium states of the nonhomogeneous elastic solid, this difficulty can be removed.

Now consider two independent equilibrium states of the elastically deformed bimaterial body. Associated field variables are denoted by superscripts 1 and 2. Superposition of the two equilibrium states leads to another equilibrium state, 0. The J integral for the superimposed state can be shown[16] to have the form

$$J^{(0)}=J^{(1)}+J^{(2)}+M^{(1,2)} \tag{13}$$

in which

$$M^{(1,2)}=\int_\Gamma \left(W^{(1,2)}\mathrm{d}x_2-\left[T_i^{(1)}\frac{\partial u_i^{(2)}}{\partial x_1}+T_i^{(2)}\frac{\partial u_i^{(1)}}{\partial x_1}\right]\mathrm{d}s\right) \tag{14}$$

where $W^{(1,2)}$ is the mutual potential energy density of the nonhomogeneous body defined by

$$W^{(1,2)}=C_{ijk\ell}u_{i,j}^{(1)}u_{k,\ell}^{(2)}=C_{ijk\ell}u_{i,j}^{(2)}u_{k,\ell}^{(1)} \tag{15}$$

Recalling the J-K relationship in Eq. (10) and the orthogonality of stress intensity factors, one can express the J integral for the new state by

$$J^{(0)}=\alpha([K_I^{(1)}+K_I^{(2)}]^2+[K_{II}^{(1)}+K_{II}^{(2)}]^2) \tag{16}$$

More explicitly, Eq. (16) can be written as

$$J^{(0)}=J^{(1)}+J^{(2)}+2\alpha(K_I^{(1)}K_I^{(2)}+K_{II}^{(1)}K_{II}^{(2)}) \tag{17}$$

A direct comparison between Eqs. (13) and (17) leads to

$$M^{(1,2)}=2\alpha[K_I^{(1)}K_I^{(2)}+K_{II}^{(1)}K_{II}^{(2)}] \tag{18}$$

The M integral in Eqs. (14) and (18) deals with interaction terms only, and will be used directly in solving the interfacial crack problem. The integral is related to the details of the stresses and deformation at the crack tip [i.e., K_I and K_{II} in Eq. (18)], but yet can be evaluated in a region away from the crack tip [i.e., the integral in Eq. (14)], where such a calculation can be carried out with greater accuracy and convenience than near the crack tip.

III. Solution Procedure

Equation (14) together with Eq. (18) provides, in fact, sufficient information for determining the stress intensity solutions $K_I^{(1)}$ and $K_{II}^{(1)}$ for the mixed-mode interfacial crack problem, when proper auxiliary solutions are introduced. Denote the first auxiliary solution by a superscript *2a*. For an interfacial crack in a body of dissimilar materials subjected to mode I deformation only, i.e.,

$$K_I^{(2a)}=1 \qquad \text{and} \qquad K_{II}^{(2a)}=0 \tag{19}$$

Equation (18) can be simplified as

$$M^{(1,2a)}=2\alpha K_I^{(1)} \tag{20}$$

where $M^{(1,2a)}$ has the form

$$M^{(1,2a)}=\int_\Gamma \left(C_{ijk\ell}u_{i,j}^{(1)}u_{k,\ell}^{(2a)}\mathrm{d}x_2 - \left[T_i^{(1)}\frac{\partial u_i^{(2a)}}{\partial x_1}+T_i^{(2a)}\frac{\partial u_i^{(1)}}{\partial x_1}\right]\mathrm{d}s\right) \tag{21}$$

and $T_i^{(1)}$ and $u_i^{(1)}$ in Eq. (21) can be determined along an arbitrarily selected integration path, Γ. Any convenient method such as the commonly used finite-element analysis, which can provide an accurate far-field solution, is suitable for this purpose. For a plane strain crack problem with the loading of Eq. (19), $T_i^{(2a)}$ and $u_i^{(2a)}$ are derivable by the Kolosov-Muskhelishvili formulation and have the forms:

$$u_i^{(2a)}=\sqrt{\frac{r}{2\pi}}f_i^{(I)}(\ell n r,\theta;G_1,\nu_1,G_2,\nu_2) \tag{22}$$

and

$$T_i^{(2a)}=\sigma_{ij}^{(2a)}n_j \tag{23}$$

with

$$\sigma_{ij}^{(2a)}=\frac{1}{\sqrt{2\pi r}}g_{ij}^{(I)}(\ell n r,\theta;G_1,\nu_1,G_2,\nu_2)+0(1) \tag{24}$$

Exact forms of the functions $f_i^{(I)}$ and $g_{ij}^{(I)}$ can be found in Refs. 8, 18, and 19.

The second auxiliary solution is denoted by the superscript *2b* for a pure mode II deformation of the nonhomogeneous solid with

$$K_I^{(2b)}=0 \qquad \text{and} \qquad K_{II}^{(2b)}=1 \tag{25}$$

Substituting Eq. (25) into Eq. (18), one obtains the following relationship

$$M^{(1,2b)}=2\alpha K_{II}^{(1)} \tag{26}$$

where

$$M^{(1,2b)}=\int_\Gamma \left(C_{ijk\ell}u_{i,j}^{(1)}u_{k,\ell}^{(2b)}\mathrm{d}x_2 - \left[T_i^{(1)}\frac{\partial u_i^{(2b)}}{\partial x_1}+T_i^{(2b)}\frac{\partial u_i^{(1)}}{\partial x_1}\right]\mathrm{d}s\right) \tag{27}$$

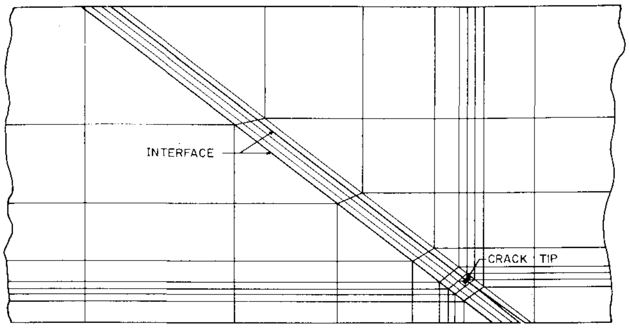

Fig. 3a Schematic finite-element mesh configuration around interfacial crack and adhesive layer.

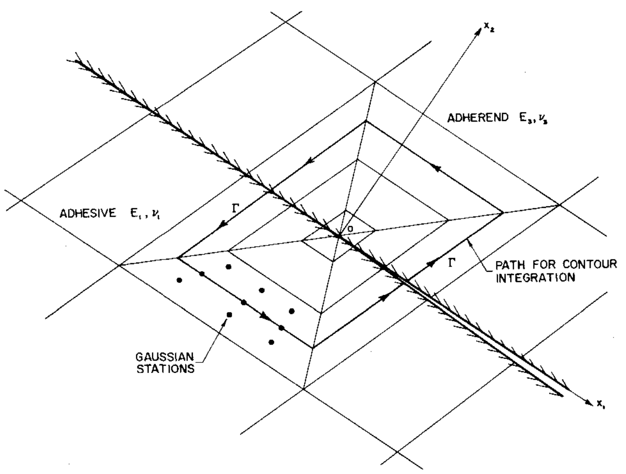

Fig. 3b Path for contour integration and finite-element mesh arrangement in crack-tip region.

The auxiliary solutions $u_i^{(2b)}$ and $T_i^{(2b)}$ have the form

$$u_i^{(2b)} = \sqrt{\frac{r}{2\pi}}\, f_i^{(II)}(\ell n r, \theta; G_1, \nu_1, G_2, \nu_2) \tag{28}$$

and

$$T_i^{(2b)} = \sigma_{ij}^{(2b)} n_j \tag{29}$$

where

$$\sigma_{ij}^{(2b)} = \frac{1}{\sqrt{2\pi r}}\, g_{ij}^{(II)}(\ell n r, \theta; G_1, \nu_1, G_2, \nu_2) + O(1) \tag{30}$$

It is important to note that the auxiliary solutions, $u_i^{(2a)}$, $T_i^{(2a)}$ and $u_i^{(2b)}$, $T_i^{(2b)}$, are independent of the particular boundary-value problem being posed. Therefore, they can be determined independently by any convenient analytical method once and for all. In solving for $K_I^{(1)}$ and $K_{II}^{(1)}$ from Eqs. (20), 21), (26), and (27), one must evaluate the integrals $M^{(1,2a)}$ and $M^{(1,2b)}$ accurately and explicitly. For a given joint geometry, loading condition, and material constants, the evaluation can be made by integrating Eqs. (21) and (27) along a properly selected contour in the far field in order to avoid crack-tip complications. A numerical method, using a conventional finite-element approach, is currently employed to calculate $T_i^{(1)}$ and $u_i^{(1)}$. The M integral is then evaluated by a numerical integration scheme using the second-order Gaussian quadrature along a properly selected contour path Γ away from the crack tip.

IV. Numerical Results and Discussions

The solution procedure outlined in Sec. III has been programmed for studying general two-dimensional interfacial crack problems in adhesively bonded joints. Evaluation of the conservation contour integrals is conducted in conjunction with a finite-element method by using eight-node isoparametric elements. For illustrative purposes, a typical finite-element mesh for a scarf joint consisting of 182 elements used in actual computation is shown schematically in Fig. 3a in the neighborhood of the adhesive bond region containing the interfacial crack. The detailed element arrangement around the crack tip and the path selected for contour integration are given in Fig. 3b. The path independency of the conservation integrals, J and M, has been checked numerically by using different paths of integration. Due to the inherently singular nature of the problem and the cumulative nature of errors introduced by the numerical analysis, proper selection of the path for integration removed enough from the crack tip is essential to insure the path independency of the contour integrals. Numerical details regarding the choice of the path are discussed in several related papers,[11,20,21] and are not repeated here. Solutions are obtained for adhesive scarf joints with various materials and geometric variables. Accuracy and convergence of the results are affected by several unusual features of the problem and the method of analysis due to the singular nature of the crack and inherent approximation in the numerical evaluation of the integrals. Assessments of the solution accuracy are made by examining relevant problems for which unquestionably correct and exact solutions are available in the literature. Excellent agreement is observed between current results and reference solutions. Details of the study are reported elsewhere.[11,20] The current results, based on the optimum mesh arrangement and the integration contour selected, have an accuracy within approximately 3% deviation from the reference solutions.

Now consider an adhesively bonded scarf joint containing an interfacial crack subjected to a unit in-plane nominal stress, σ_∞ [i.e., $\sigma_\infty = 6.895 \times 10^3$ Pa (1 psi)], as shown in Figs. 1a and 1b. The adherends in the composite structure have a uniform thickness $d = 1.27$ cm (0.5 in.) and a total length of $2L = 25.4$ cm (10 in.). For simplicity without loss of generality, the scarf angle ϕ of the joint is taken as 45 deg for illustrative purposes (ϕ is generally smaller than 45 deg in most practical cases). The adherends are structural aluminum with elastic constants typical for aircraft construction

$$E_2 = E_3 = 6.895 \times 10^4 \text{ MPa } (10 \times 10^6 \text{ psi})$$

and

$$\nu_2 = \nu_3 = 0.33$$

Effects of geometric and material variables of the thin adhesive layer and the interfacial crack on the fracture behavior of the joints are the subject under current investigation. The primary objectives of this section are to examine the complex failure modes and mechanics associated with an interfacial crack and to assess the influence of problem variables on the crack-tip behavior in adhesively bonded scarf joints. Mixed-mode stress intensity factor solutions and associated energy release rates, which characterize the stresses and deformation in the crack-tip region, are evaluated for various cases. The reduction of structural stiffness of the joint due to the presence of an edge interfacial crack is also studied to illustrate the significance of the defect on structural integrity. Of particular interest is the crack-tip response in the joints with different bond thicknesses; quantitative information on this important subject is determined. In the following numerical examples, the plane strain condition is assumed for all of the interfacial crack problems.

A. Effect of Adhesive Material Property

Effects of different kinds of adhesive on the crack-tip response in the joints are examined by considering adhesives

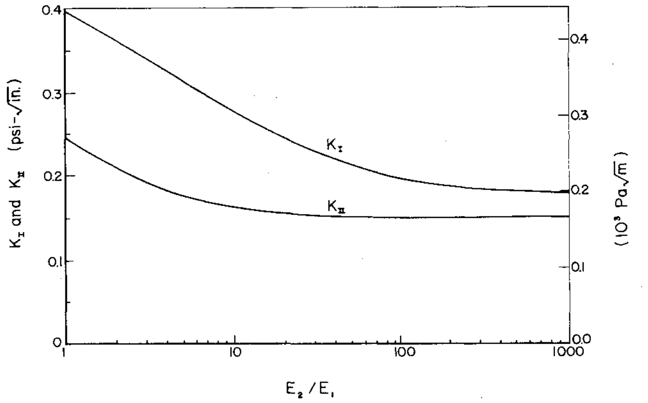

Fig. 4 Effect of adhesive modulus on mixed-mode interfacial crack-tip stress intensity factors ($E_2 = E_3 = 6.895 \times 10^4$ MPa(10×10^6 psi).

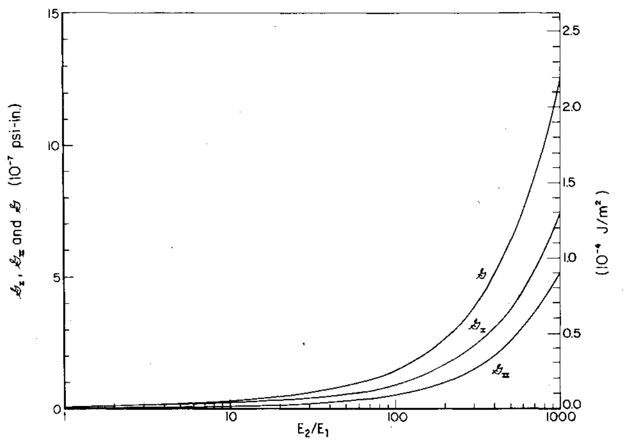

Fig. 5 Effect of adhesive modulus on energy release rates in debonded scarf joint ($E_2 = E_3 = 6.895 \times 10^4$ MPa(10×10^6 psi).

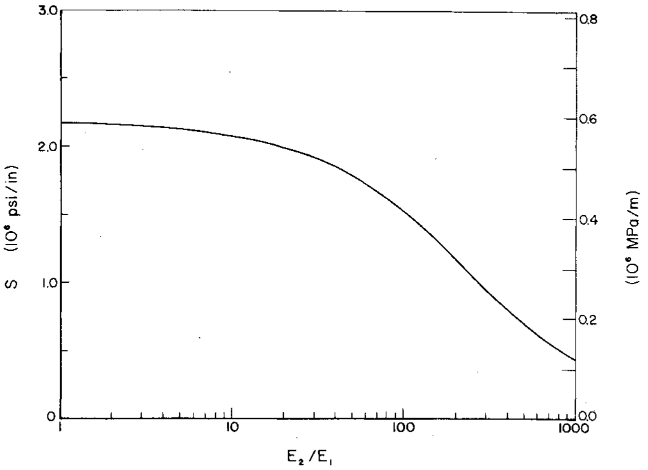

Fig. 6 Variation of structural stiffness, S, of debonded adhesive scarf joints with different E_2/E_1's ($E_2 = E_3 = 6.895 \times 10^4$ MPa(10×10^6 psi).

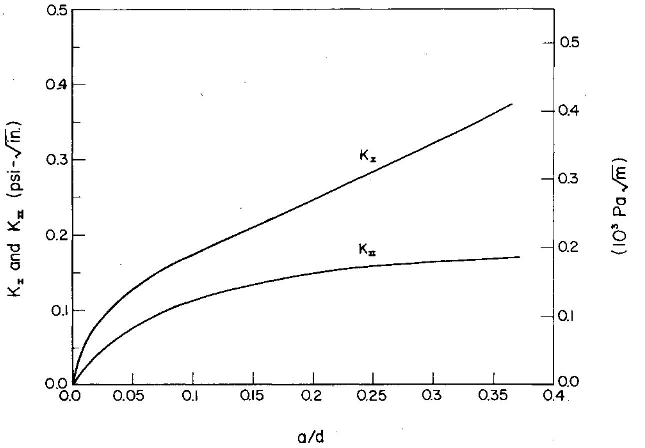

Fig. 7 Effect of interface crack length, a/d on, mixed-mode crack-tip stress intensity factors K_I and K_{II}.

with various material constants, E_1's or E_2/E_1's (with given adherends and $\nu_1 = 0.3$). For the purpose of generality, adhesives with a broad range of Young's modulus covering three decades on a logarithmic scale are studied. The cases with $E_2/E_1 = 20 \sim 40$ are typical for aluminum-epoxy composite structures. Higher E_2/E_1 values correspond to the joints with less rigid adhesives or subjected to a "hot and wet" environment. Crack-tip stress intensity factor solutions and associated energy release rates are shown in Figs. 4 and 5 as functions of the modulus ratio for the joints with $t/d = 0.05$ and $a/d = 0.2$. Failure modes and mechanics associated with the interfacially cracked joints are revealed. Obviously, the interfacial crack experiences a mixed-mode fracture even under uniaxial nominal loading, because K_I and K_{II} are of the same order of magnitude for all of the cases studied.

Both K_I and K_{II} are observed to decrease as the modulus of the adhesive decreases. The difference between K_I and K_{II} decreases with E_1 also. The mode I stress intensity factor is always higher than that of the mode II in the entire range of E_2/E_1 studied; thus, the dominant mode of failure is an opening one in the joints with the scarf angle considered. The shearing mode stress intensity factor remains relatively unchanged for most practical adhesive scarf joints with E_2/E_1 greater than 20. In the case of $E_2/E_1 = 1$, the crack is cohesive, and the nature of the crack-tip singularity changes. In this case, stress intensity solutions, K_I and K_{II}, are found to be consistent with the results given in Ref. 22. The energy release rate of each individual fracture mode, $\mathcal{G}_I$ and $\mathcal{G}_{II}$, and the total energy release rate, $\mathcal{G}$, are evaluated. For the joints with a given adherend material, alternation of adhesive properties results in a change of α in Eqs. (10-12). The reduction of E_1 increases the α value which significantly influences the $\mathcal{G}_I$, $\mathcal{G}_{II}$ and $\mathcal{G}$. Both $\mathcal{G}_I$ and $\mathcal{G}_{II}$ increase rapidly with E_2/E_1, especially as $E_2/E_1 > 20$. The rapid increase of $\mathcal{G}_I$, $\mathcal{G}_{II}$ and $\mathcal{G}$ corresponding to the decrease of K_I and K_{II} is noted to be a phenomenon uniquely associated with the interfacial crack problem, and is not observed in a homogeneous crack problem in general. In the cases of very large values of E_2/E_1, the adhesive may become incompressible with a Poisson's ratio approaching 0.5. The incompressibility of the soft adhesive is not considered in the present study.

The influence of adhesive material properties on structural integrity of debonded scarf joints is shown in Fig. 6 in which a reduction of structural stiffness, S, is observed (computed on the basis of the applied stress and resulting displacements at the ends of the joint). The joint stiffness decreases monotonically with the adhesive modulus. The stiffness reduction is found especially significant for the joints with E_2/E_1 greater than 20. For instance, an approximately 400% decrease in the joint structural stiffness is observed, as E_2/E_1 increases from 20 to 1000.

B. Influence of Interfacial Crack (Debonding) Length

The interfacial crack length is of particular interest because of its influences on failure mechanics, joint integrity, and overall performance of the bonded structure. The joints studied here have the same geometry as those examined in the previous section [i.e., $2L = 25.4$ cm(10 in.), $d = 1.27$ cm(0.5 in.), $\phi = 45$ deg, $t/d = 0.05$]. The adherends are the same aluminum, and the adhesive is a structural epoxy with material constants $E_1 = 3.448 \times 10^3$ MPa (0.5×10^6 psi) and

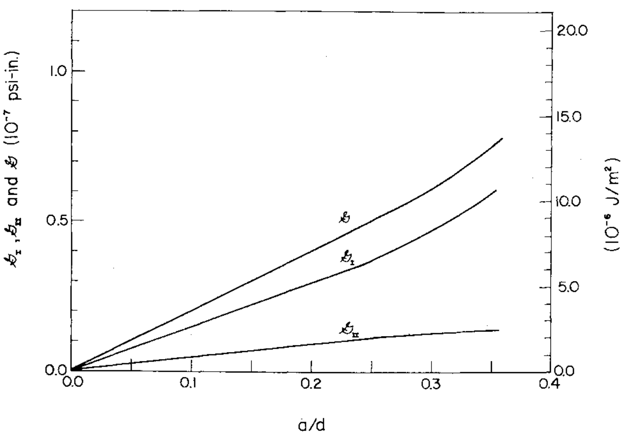

Fig. 8 Effect of interface crack length, a/d, on energy release rates, $\mathcal{G}_I$, $\mathcal{G}_{II}$ and $\mathcal{G}$ in debonded scarf joint.

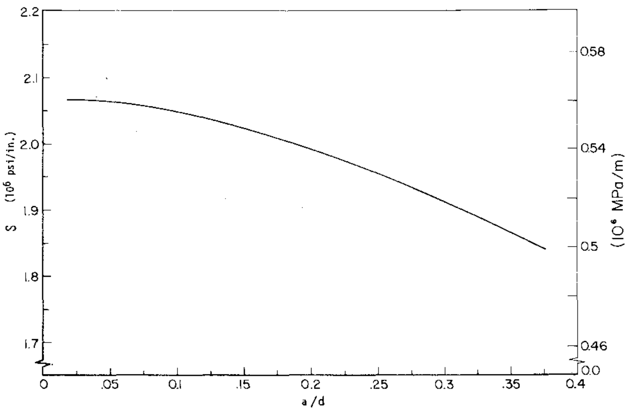

Fig. 9 Reduction of structural stiffness, S, due to the presence of interface crack, a/d, in debonded scarf joint.

$\nu_I = 0.3$. The scarf joints with interfacial crack lengths, a/d, ranging from 0.05 to 0.4 are studied in detail. Effects of a/d on mixed-mode crack-tip stress intensity factors are shown in Fig. 7. The opening mode stress intensity factor K_I increases monotonically with the debonding length. The shearing mode stress intensity K_{II} changes with the interfacial crack length in a manner similar to K_I but at a lower rate. As the debonding length exceeds $0.2d$, K_{II} becomes less sensitive to the change of a/d. The value of K_I is found increasingly larger than that of K_{II} as a/d increases. Hence, the larger the debonding length, the more dominant the opening mode fracture in the joint. Corresponding energy release rates in the joints with various interfacial crack lengths are reported in Fig. 8. As anticipated, $\mathcal{G}_I$, $\mathcal{G}_{II}$ and $\mathcal{G}$ change with the crack length in an approximately linear manner. Slight deviation from linearity occurs as a/d becomes large. The mode II energy release rate $\mathcal{G}_{II}$ is observed to increase with a smaller gradient as compared with that of $\mathcal{G}_I$. The associated structural stiffness change of the joint is evaluated also and shown in Fig. 9. As one expects, increasing the interfacial crack length leads to a gradual reduction of joint stiffness. For example, a change of debonding length a/d from 0.1 to 0.4 causes a 15% decrease in structural stiffness.

C. Effect of Adhesive-Layer Thickness

Effects of the adhesive-layer thickness on fracture of bonded joints have long been recognized. Bascom et al.,[5] for example, showed experimentally that fracture energy release rates were related closely to the bond thickness, indicating the criticality of the adhesive thickness in controlling the failure of structural joints. Erdogan et al.[2,23] conducted analytical studies on crack-tip stresses in debonded composite laminates and reported unique features of this geometric variable in the joint fracture behavior. Wang et al.[24,25] examined center-of-the-bond cohesive cracks and showed fundamental characteristics of thickness effects of the adhesive layer on fracture of the joints. In this portion of the study, scarf joints containing an interfacial crack of $a/d = 0.2$ with various adhesive-layer thicknesses, t/d, ranging from 0.01 to 0.1 [i.e., $t = 0.127 \sim 1.27$ mm(0.005-0.05 in.)] are considered. Other geometric variables and materials properties are identical to those used in previous sections.

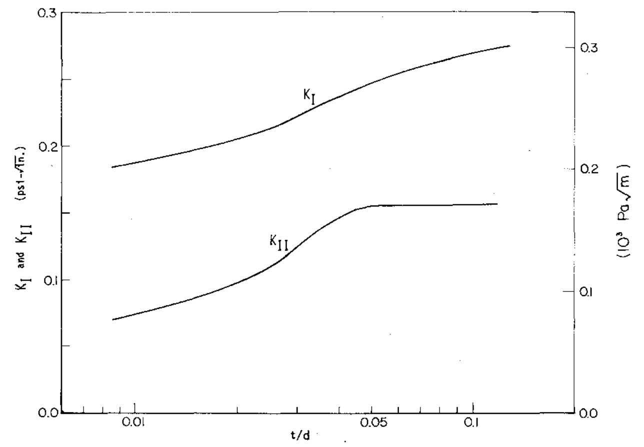

Fig. 10 Effect of adhesive layer thickness, t/d, on interface crack-tip stress intesity factors K_I and K_{II}.

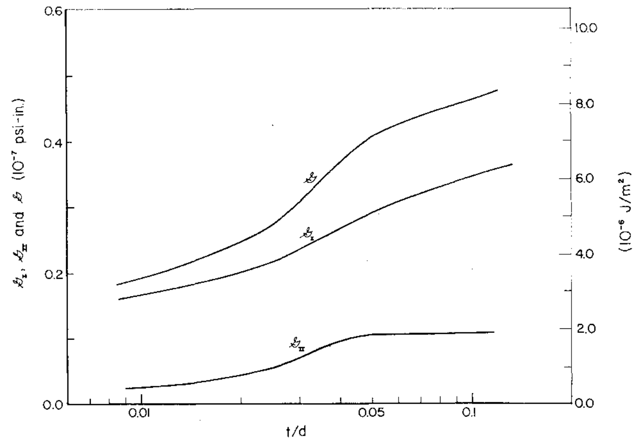

Fig. 11 Effect of adhesive layer thickness, t/d, on energy release rates, $\mathcal{G}_I$, $\mathcal{G}_{II}$ and $\mathcal{G}$ in debonded scarf joint.

Relationships among K_I, K_{II}, and the bond thickness are shown in Fig. 10. The opening mode stress intensity solution is found to increase initially with the adhesive-layer thickness. As t/d becomes very large, K_I and K_{II} must approach an asymptotic value for the interfacial crack between two dissimilar materials, i.e., the adhesive E_I and the adherend E_3. The shearing mode stress intensity factor increases with t/d first, and then becomes less sensitive to the change of the bond thickness as t exceeds a certain value (i.e., $t/d = 0.05$ in this case). The opening mode stress intensity factor is always larger than that of the shearing mode in all cases studied; thus, the mode I failure becomes increasingly critical as the adhesive thickness increases. Associated energy release rates for the joints with various t/d's are given in Fig. 11. With a given debonding length, the decrease of the adhesive-layer thickness leads to an increase of fracture resistance in the bonded joints (i.e., a reduction in the total energy release rate and in the maximum cleavage stress). The change of fracture resistance with the bond thickness is of critical importance in the fracture design of adhesively bonded structures. This finding is consistent with the results reported by Erdogan.[23] However, variations of interfacial crack-tip stress intensity factors and associated energy release rates with t/d in the current problem are in contrast to the solutions obtained for center-of-the-bond cohesive crack problems in which K's and $\mathcal{G}$'s are found to be almost independent of the adhesive-layer thickness. This situation is expected as the associated stress singularities are quite different between the two cases,[24] and the stress intensity factors of an interfacial crack are defined differently from those of a cohesive one.

V. Summary and Conclusions

Interfacial cracks in adhesively bonded scarf joints are studied with a method of analysis based on conservation laws in elasticity for nonhomogeneous solids and fundamental relationships of fracture mechanics for interfacial crack problems. The current approach is shown to provide an effective and efficient means to examine the complex interfacial crack behavior and the performance of debonded joints. Solutions are obtained for scarf joints containing an edge interfacial crack with various adhesive types, debonding lengths, and adhesive-layer thicknesses. Fracture parameters such as mixed-mode stress intensity factors and associated energy release rates describing the crack-tip stresses and deformation are determined. Influences of material and geometric variables on the integrity of the bonded structures are also studied.

Based on the results obtained in the study, the following conclusions can be drawn:

1) The current method of analysis is superior to other approaches in its operational simplicity and solution accuracy for studying mixed-mode interfacial crack problems in adhesive joints with complex geometries.

2) The change of adhesive material properties significantly influences the interfacial crack-tip response and joint performance. In the scarf joints studied, the opening mode stress intensity factor is always greater than that of the shearing mode, and the difference between K_I and K_{II} decreases with the increase of E_2/E_1. The associated energy release rates increase rapidly with the decrease of crack-tip stress intensity factors as E_2/E_1 increases—a phenomenon unique to the interfacial crack behavior in a nonhomogeneous solid and not observed in homogeneous crack problems in general. The structural stiffness of a debonded joint decreases rapidly as E_2/E_1 becomes greater than 20.

3) Increasing the interfacial crack length in scarf joints raises K_I and K_{II} simultaneously. The magnitude and the rate of change of K_I are considerably larger than those of K_{II}. As the crack length increases, K_{II} becomes gradually insensitive to a/d, but K_I increases monotonically. Energy release rates associated with the interfacial crack increase approximately linearly with the crack length, but deviation from linearity starts as the crack length a/d exceeds 0.3. The structural stiffness of the joint decreases appreciably with a/d.

4) Effects of the adhesive-layer thickness on the interfacial crack response are significant. Both K_I and $\mathcal{G}_I$ increase monotonically with the change of the adhesive thickness initially, and approach their asymptotic values, which are the mode I stress intensity and energy release rate for an interfacial crack in two dissimilar materials, as t/d becomes very large. But K_{II} and $\mathcal{G}_{II}$ become relatively insensitive to the increase of t/d as the adhesive layer exceeds a certain thickness. The increase of the adhesive bond thickness leads to a decrease of fracture resistance of the joint in general.

Acknowledgments

The work reported in this paper was supported in part by the Office of Naval Research through Contract N00014-79-C-0579. Computation was carried out in the Digital Computer Laboratory of the University of Illinois at Urbana-Champaign. The authors are grateful to Dr. N. Perrone of ONR for his encouragement and cooperation during the course of this study. Fruitful discussion with Dr. D. L. Hunston of the Naval Research Laboratory, Washington, D. C., is also gratefully acknowledged.

References

[1] Bikerman, J. J., *The Science of Adhesive Joints*, Academic Press, New York, 1968, pp. 234-235.

[2] Erdogan, F. and Gupta, G. D., "Layered Composites with an Interfacial Flaw," *International Journal of Solids and Structures*, Vol. 7, Aug. 1971, pp. 1089-1107.

[3] Gecit, M. R. and Erdogan, F., "The Effect of Adhesive Layer on Crack Propagation in Laminates," NASA Tech. Rept., Grant NGR 39-007-011, Dept. of Mechanical Engineering and Mechanics, Lehigh Univ., March 1976.

[4] Bascom, W. D., Timmons, C. O., and Jones, R. L., "Apparent Interfacial Failure in Mixed-Mode Adhesive Fracture," *Journal of Materials Science*, Vol. 10, June 1975, pp. 1037-1048.

[5] Bascom, W. D., Cottington, R. L., Jones, R. L., and Peyser, P., "The Fracture of Epoxy- and Elastomer-Modified Epoxy Polymers in Bulk and as Adhesives," *Journal of Polymer Science*, Vol. 19, Nov. 1975, pp. 2545-2562.

[6] Williams, M. L., "The Stress Around a Fault or Crack in Dissimilar Media," *Bulletin of the Seismological Society of America*, Vol. 49, No. 2, June 1959, pp. 199-204.

[7] England, A. H., "A Crack Between Dissimilar Media," *Journal of Applied Mechanics*, Vol. 32, No. 2, June 1965, pp. 400-411.

[8] Rice, J. and Sih, G. C., "Plane Problems of Cracks in Dissimilar Media," *Journal of Applied Mechanics*, Vol. 32, No. 2, June 1965, pp. 418-423.

[9] Williams, M. L., "The Relation of Continuum Mechanics to Adhesive Fracture," *Journal of Adhesion*, Vol. 4, No. 4, Aug. 1972, pp. 307-332.

[10] Smelser, R. E. and Gurtin, M. E., "On the J-Integral for Bimaterial Bodies," *International Journal of Fracture*, Vol. 13, No. 3, June 1977, pp. 382-386.

[11] Wang, S. S. and Yau, J. F., "Analysis of Interfacial Cracks Based on Conservation Laws in Elasticity," to appear in *International Journal of Solids and Structures*, 1981.

[12] Wang, S. S. and Yau, J. F., "An Analysis of Interface Cracks in Adhesively Bonded Lap-Shear Joints," *Modern Developments in Composite Materials and Structures*, edited by J. R. Vinson, American Society of Mechanical Engineers, Dec. 1979, pp. 67-83.

[13] Eshelby, J. D., "The Continuum Theory of Lattice Defects," *Solid State Physics*, Vol. 3, edited by F. Seitz and D. Turnbull, Academic Press, New York, 1956, pp. 79-144.

[14] Knowles, J. K. and Sternberg, E., "On a Class of Conservation Laws in Linearized and Finite Elastostatics," *Archive for Rational Mechanics and Analysis*, Vol. 44, No. 3, 1972, pp. 187-211.

[15] Budiansky, B. and Rice, J., "Conservation Laws and Energy Release Rates," *Journal of Applied Mechanics*, Vol. 40, No. 1, March 1973, pp. 201-203.

[16] Chen, F. H. K. and Shield, R. T., "Conservation Laws in Elasticity of the J-Integral Type," *Journal of Applied Mathematics and Physics (ZAMP)*, Vol. 28, No. 1, March 1977, pp. 1-22.

[17] Muskhelishvili, N. I., *Some Basic Problems of Mathematical Theory of Elasticity*, Noordhoff, Groningen, The Netherlands, 1953.

[18] Malyshev, B. M. and Salganik, R. L., "The Strength of Adhesive Joints Using the Theory of Cracks," *International Journal of Fracture Mechanics*, Vol. 1, No. 2, June 1965, pp. 114-128.

[19] Erdogan, F., "Stress Distribution in Bonded Dissimilar Material with Cracks," *Journal of Applied Mechanics*, Vol. 32, No. 2, June 1965, pp. 403-410.

[20] Yau, J. F., Wang, S. S., and Corten, H. T., "A Mixed-Mode Crack Analysis of Isotropic Solids, Using Conservation Laws of Elasticity," *Journal of Applied Mechanics*, Vol. 47, No. 2, June 1980, pp. 335-341.

[21] Wang, S. S., Yau, J. F., and Corten, H. T., "A Mixed-Mode Crack Analysis of Rectilinear Anisotropic Solids Using Conservation Laws of Elasticity," *International Journal of Fracture*, Vol. 16, No. 3, June 1980, pp. 247-259.

[22] Wilson, W. K., "On Combined Mode Fracture Mechanics," Res. Rept. 69-1E7-EMECM-R1, Westinghouse Research Labs., Pittsburgh, Pa., June 1969.

[23] Erdogan, F., "Fracture Problems in Composite Materials," *Engineering Fracture Mechanics*, Vol. 4, No. 4, Dec. 1972, pp. 811-840.

[24] Wang, S. S., Mandell, J. F., and McGarry, F. J., "An Analysis of the Crack-Tip Stress Field in DCB Adhesive Fracture Specimens," *International Journal of Fracture*, Vol. 14, No. 1, Feb. 1978, pp. 39-58.

[25] Wang, S. S., "An Analysis of Tapered Double-Cantilever-Beam Fracture Toughness Tests for Adhesive Joints," *Fracture Mechanics ASTM STP 677*, edited by C. W. Smith, American Society for Testing and Materials, 1979, pp. 651-667.